Functional biomimetic models for the active site in the respiratory enzyme cytochrome c oxidase

James P. Collman* and Richard A. Decréau

Received (in Cambridge, UK) 12th May 2008, Accepted 30th July 2008
First published as an Advance Article on the web 4th September 2008
DOI: 10.1039/b808070b

A functional analog of the active site in the respiratory enzyme, cytochrome c oxidase (CcO) reproduces every feature in CcO's active site: a myoglobin-like heme (heme *a3*), a distal tridentate imidazole copper complex (Cu_B), a phenol (Tyr244), and a proximal imidazole. When covalently attached to a liquid-crystalline SAM film on an Au electrode, this functional model continuously catalyzes the selective four-electron reduction of dioxygen at physiological potential and pH, under rate-limiting electron flux (as occurs in CcO).

Background

Metalloenzymes that catalyze multi-electron redox reactions are essential to life on earth. Significant examples are found in respiration,[1a–c] photosynthesis,[2a,b] and nitrogen fixation.[3a–c] The symbiotic relationship that takes place between photosynthesis in chloroplasts[2a,b] and respiration in mitochondria[1] illustrated in Fig. 1 shows the broad significance of these enzymes. In each process the terminal step is catalyzed by metallic enzymes. In chloroplasts energy derived from sunlight is used to convert carbon dioxide into carbohydrates while releasing molecular oxygen as a byproduct from oxidation of water.[2a,b] In the mitochondria electrons derived from the three natural food groups: carbohydrates, proteins and fats, combine with oxygen to produce water and energy in the form of ATP and heat while releasing carbon dioxide as a byproduct.[1a–c]

Stanford University, Chemistry Department, Stanford, CA-94305-5080, USA. E-mail: jpc@stanford.edu; Fax: +00 1 650 725; Tel: 00 1 650 725 0000

The redox enzymes, shown in Fig. 2, each contain several metal centers. The detailed mechanisms involved in these multi-electron redox processes are not well understood, but it is clear that the metal centers in the enzyme active sites play several roles: they bind the substrate, increase its reactivity, suppress side reactions, and rapidly transfer electrons.[1–3] One of the most challenging goals of modern chemistry is to synthesize analogs of these multi-electron redox enzymes that will exhibit similar catalytic activity.

A functional mimic of CcO's active site

As discussed in this account, our research has focused on the invention, synthesis, and catalytic studies of such functional models for the active site in cytochrome c oxidase, CcO.[4a–k] During respiration, CcO reduces molecular oxygen to water, a four-electron process, while avoiding the escape of toxic, partially reduced oxygen species, PROS, such as superoxide, peroxide and hydroxy radicals.[1a–c] Fig. 3 gives a metabolic overview of the processes that occur during respiration.

James P. Collman

James P. Collman was born in 1932 and received BS and MS degrees from the University of Nebraska in 1954 and 1956, and a PhD from the University of Illinois in 1958 under the supervision of R. C. Fuson. In 1958–1967 he was on the faculty of the University of North Carolina at Chapel Hill; he moved to Stanford in 1967, where he is Daubert Professor of Chemistry. His research interests are very broad, extending across inorganic and organic chemistry, and also include superconductivity. His principal research is directed toward the development of structural and functional analogues of the active sites in heme proteins, particularly cytochrome oxidase. His work has been recognized by many awards; he is a member of the National Academy of Sciences.

Richard A. Decréau

Richard A. Decréau graduated from Aix-Marseille University (France) in 1998, studying Photodynamic Therapy on Melanoma in Prof. Michel Chanon's group. In 1999–2000 he did a postdoc at University College London (Britain) in Prof. Charles M. Marson's group, studying steroid biotransformations. With a Lavoisier Fellowship he moved to Stanford University (USA) and worked in Prof. James P. Collman's group, as a Postdoc and thereafter as a Research Associate. The major focus of his current research is the synthesis and reactivity studies of biomimetic models of several hemoprotein active sites. He is currently managing the Collman group.

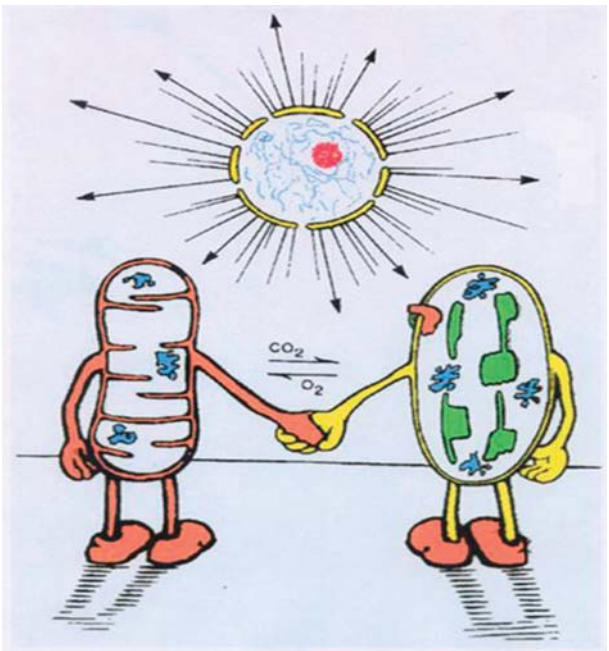

Fig. 1 The symbiotic interaction between mitochondria (left) and chloroplasts (right).

- Often possess **multiple** metal centers
- Metals play multiple roles
  1. **Bind substrate**
  2. **Increase reactivity of substrate**
  3. **Prevent side reaction**
  4. **Provide electrons quickly**
- Couple a **multielectron** process to several **single** electron processes

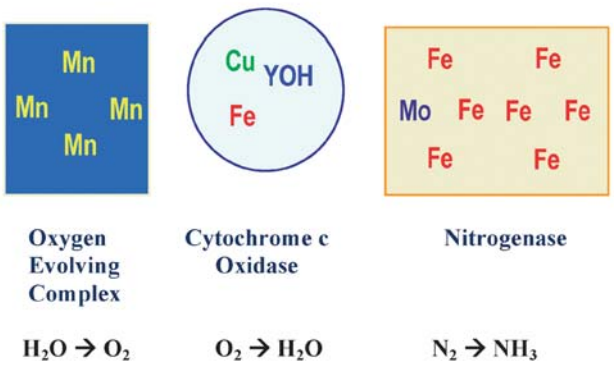

Fig. 2 Multielectrons redox enzymes.

An array of anaerobic reactions transform the three food groups, fats, carbohydrates, and proteins into acetyl CoA, which engages in the citric acid cycle producing carbon dioxide and electrons.[1a–c] These electrons are transported to the mitochondria by cytochrome c where oxygen is reduced and ATP is formed. The latter process is referred to as oxidative phosphorylation.[1a–c]

A cartoon illustrating the membrane-bound CcO is shown in Fig. 4. The enzyme active site contains Fe, Cu, and a phenol

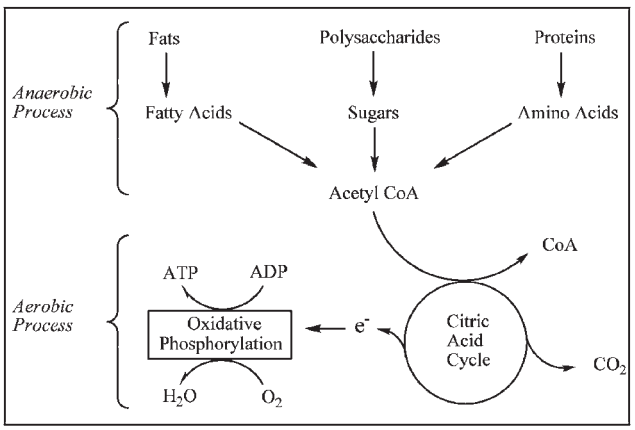

Fig. 3 A metabolic overview.

(YOH). Oxygen is reduced by four electrons to water at this site, but each electron is delivered one at a time from external cytochrome c. Four protons are required for oxygen reduction to water, but simultaneously up to four additional protons are pumped to the outside of the membrane. The energy generated by this exergonic reaction can be accounted for as heat and a proton gradient.[1a–c,5a–d]

Fig. 5 shows a more detailed view of CcO. Each of the functional parts of this enzyme are illustrated: a binuclear copper site, "Cu_A", a coordinatively saturated heme, "heme *a*", and in the active site where oxygen is reduced, a myoglobin-like heme *a3*.[6a–e] Note also a coordinatively unsaturated distal copper, Cu_B that lies close to heme *a3* in the site where oxygen is reduced. This figure does not show the reactive phenol, "Tyr244". A complex array of intervening protein structures are involved in electron transfers and the proton pumping. Finally, cytochrome c is depicted delivering an electron to the Cu_A site.

Fig. 6 displays another simplified diagram of CcO. The redox active groups, Cu_A, heme *a*, and the two groups at the active site: heme *a3* and Cu_B are illustrated as well as the four-electron reduction of oxygen and the proton pump.

At the left side of Fig. 6 the production of ATP from ADP and phosphate is illustrated as the proton gradient is relaxed by protons flowing through another enzyme ATPase, which is also embedded in the membrane.[1a,7a] A constant supply of ATP is required to drive many of the functions that living aerobic systems depend upon: muscle action, nerve impulses, *etc*.[7b] An average adult may produce as much as 34 kg of ATP

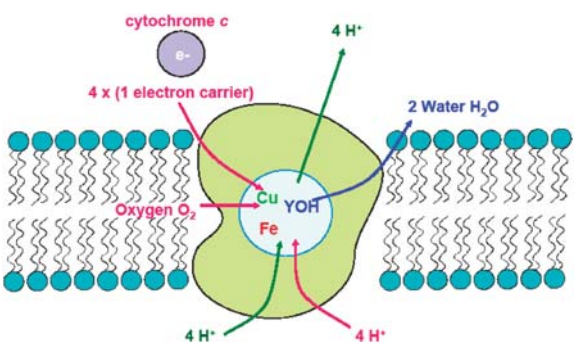

Fig. 4 Cytochrome c oxidase, a membrane-bound enzyme.

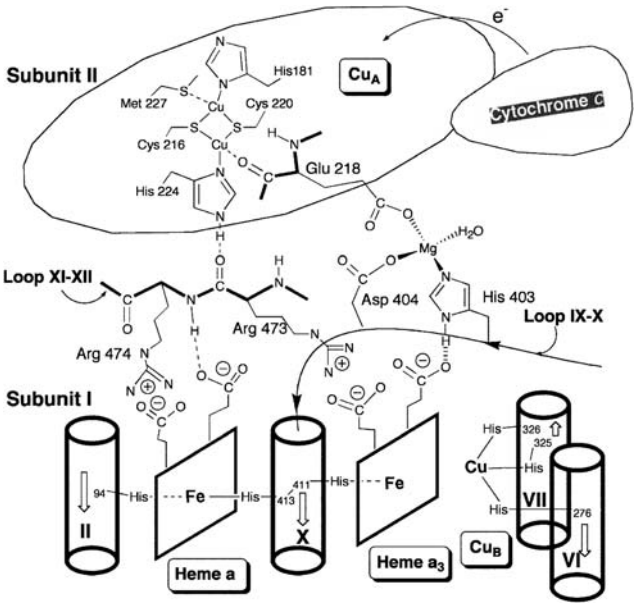

Fig. 5 Schematic view of CcO in the mitochondrial inner membrane.

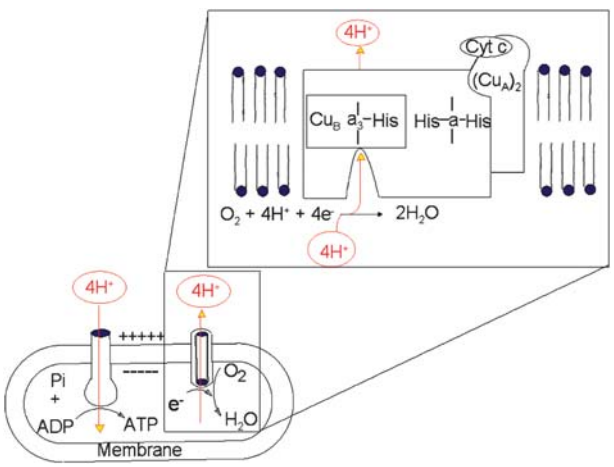

Fig. 6 Schematic diagram of cytochrome c oxidase.

during a 24 h period. Termination of respiration by inhibitors would cut off ATP production resulting in death.[1c,7a,b]

A structure of the essential groups at the active site of CcO is shown on the upper right hand side of Fig. 7. This structure was derived from X-ray diffraction studies.[6a–e] Note the presence of a phenol that is covalently attached to one of the imidazole ligands in Cu_B. This phenol is derived from a tyrosine, referred to as Tyr244, and it is cross-linked to an histidine. It is formed post-translationally and is present in most functional CcO's.[6a–e,8a–c]

A list of the five possible oxidation states for each of the redox-active metal sites at the active site is given at the bottom of Fig. 7. In the fully oxidized enzyme, Cu_A and Cu_B both exist as Cu(II), whereas both Fe*a* and Fe*a3* are Fe(III).[1a–c,9a] This fully oxidized form does not react with oxygen. Recall two conditions are necessary for a metal to bind oxygen. The metal must be coordinatively unsaturated so the oxygen ligand has a

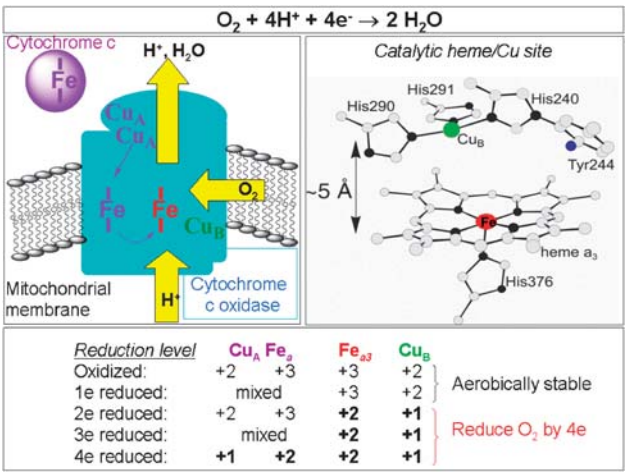

Fig. 7 Cytochrome c oxidase couples diffusional 1e oxidation of ferrocytochrome c to rapid 4e reduction of O_2. Four redox states of the enzyme are listed.

place to bind (this is the situation in both Fe*a3* and Cu_B. Second, the metal must be capable of donating an electron to oxygen, as are Fe(II) and Cu(I), but not Fe(III) and Cu(II). The resulting superoxide ion binds to the unsaturated, but oxidized metal. When one electron is added to the fully oxidized enzyme, it is shared equally between Cu_A and Fe*a*, apparently by oscillating between these two metal centers. This one-electron reduced form is aerobically stable because neither of the reduced metals is coordinatively unsaturated. Addition of a second electron results in an unusual situation. This doubly-reduced state acts as if both electrons are present at the active site such that Fe*a3* and Cu_B are in the Fe(II), and Cu(I) states. This doubly reduced state reacts with oxygen and rapidly reduces it by four electrons! Because electrons arriving from Cyt c are delivered, one at a time to CcO at a very slow rate, compared with the very rapid internal electron transfers that take place within CcO during the steady-state reduction of oxygen, this doubly reduced state predominates during catalytic turnover. When oxygen is present the enzyme never receives more than two electrons.[9a,b] However, in the absence of oxygen it is possible to create two additional redox states, which contain three and four total electrons, respectively. These more highly reduced states can also reduce oxygen to water, but these states are not relevant to the steady-state turnover of CcO. As will be discussed, we have carried out single turnover experiments on the biologically relevant two-electron reduced model system.

Fig. 8 illustrates the challenge of reducing oxygen to water without releasing intermediate, toxic, partially reduced oxygen species (PROS) such as superoxide, peroxide and hydroxy radicals. It was essential for aerobic organisms to develop strategies to carry out the four-electron reduction without forming such toxic PROS.[1a–c,10a,b] Our goal was to develop a model that imitates the function of CcO by catalytically reducing oxygen without producing PROS, and to understand the mechanism of this four-electron reduction under circumstances where one electron is added at a time in a rate-limiting fashion.

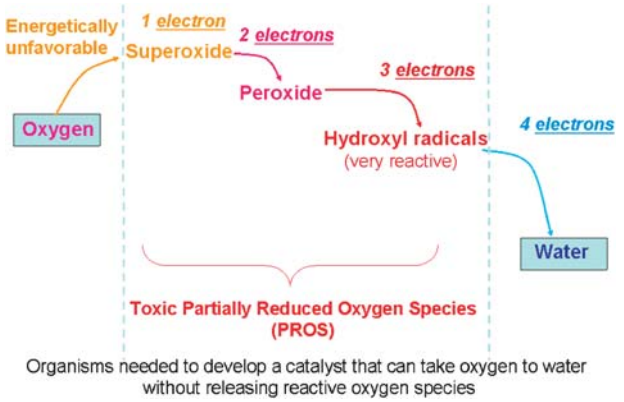

Fig. 8 The challenge of reducing oxygen.

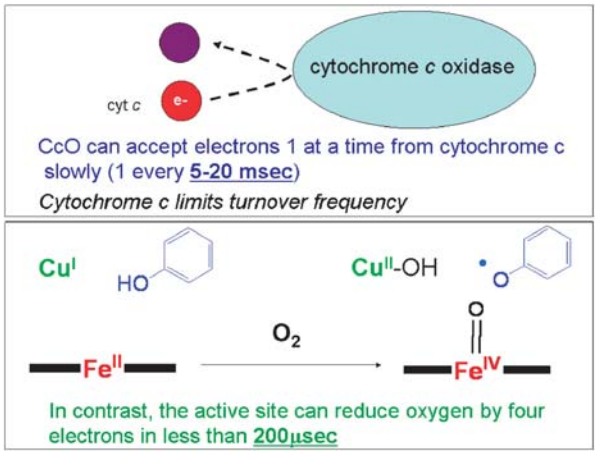

Fig. 10 Differences in electron transfer rates.

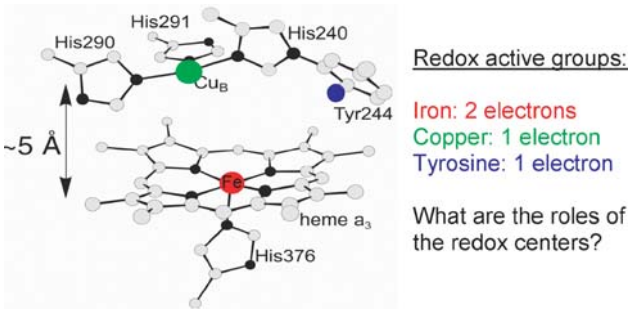

Fig. 9 Cytochrome c oxidase active site.

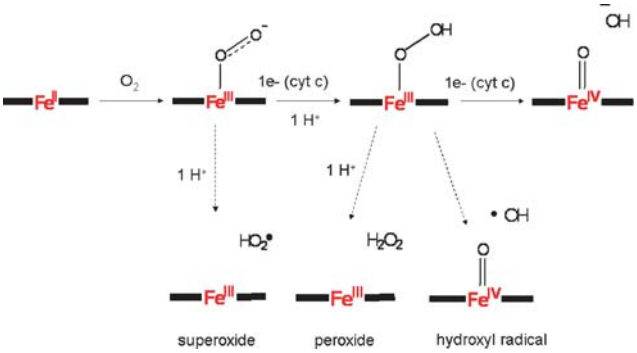

Fig. 11 The problem of waiting for external electrons.

Fig. 9 shows the four redox-active groups at the catalytic center of CcO: the heme iron, that can donate two electrons as it passes from Fe(II) to an Fe(IV) oxo, Cu_B, that can provide one electron as it goes from Cu(I) to Cu(II), and the phenol in Tyr244, which becomes a phenolate radical.[11a–g] Collectively these three redox centers can provide the four electrons necessary to convert oxygen to the level of water without releasing PROS. But how does this occur?

Control of the rate of electron flux

In order to mimic the actual situation during the steady state reduction of oxygen one must consider the rates of internal and external electron transfer. Fig. 10 illustrates dramatic differences in electron transfer rates between the slow, stepwise delivery of electrons from Cyt c and the rapid internal electron transfers within CcO itself. It is clear that during continuous catalytic reduction of oxygen electron transfer from Cyt c is rate limiting.[1a,12a–i] Ideally, a fully-functional CcO active site model should reproduce this slow, steady-state electron delivery during catalytic reduction of oxygen.

Fig. 11 illustrates the problem faced by a catalyst that must wait for external electrons before consummating the four-electron reduction of oxygen. PROS such as superoxide, peroxide and hydroxyl radicals might leak from the active site before oxygen reduction is complete. For example, hydrolysis of superoxide or peroxide intermediates would release toxic PROS. This difficulty might be overcome by four rapid electron transfers within the active site, thus minimizing the lifetime of any partially-reduced intermediate oxygen species. Using single turnover experiments with our models we have shown how this could occur.[13a,b]

As shown in Fig. 12 we began these model studies by preparing a complex that mimics the first step: binding of oxygen to the reduced active site model. The nature of the initially formed oxygen complex in CcO itself had been in dispute. It was expected that by accepting one electron from each reduced metal center oxygen would form a peroxide bridge between Fe(III) and Cu(II).[1a,14a–j] But experiments with our functional model, show that the oxygen complex, as shown in Fig. 12, does not form a bridge with Cu.[13b,15] Rather this exists as an Fe(III)/superoxide complex having a neighboring reduced Cu(I) atom. Studies of the oxygen complex formed by reduced CcO have a similar structure.[16] This surprising result contains a lesson: unless a model complex has all of the ligand components and the same geometry as the enzyme, the model structure may not mirror that of the enzyme. Two lines of experimental evidence support this hypothesis. Our oxygen complex is a diamagnetic superoxide complex as is demonstrated by its sharp ^{1}H NMR spectrum, and by the characteristic resonance enhanced Fe–O Raman frequency (both shown in Fig. 12).[13b,15] Recall that

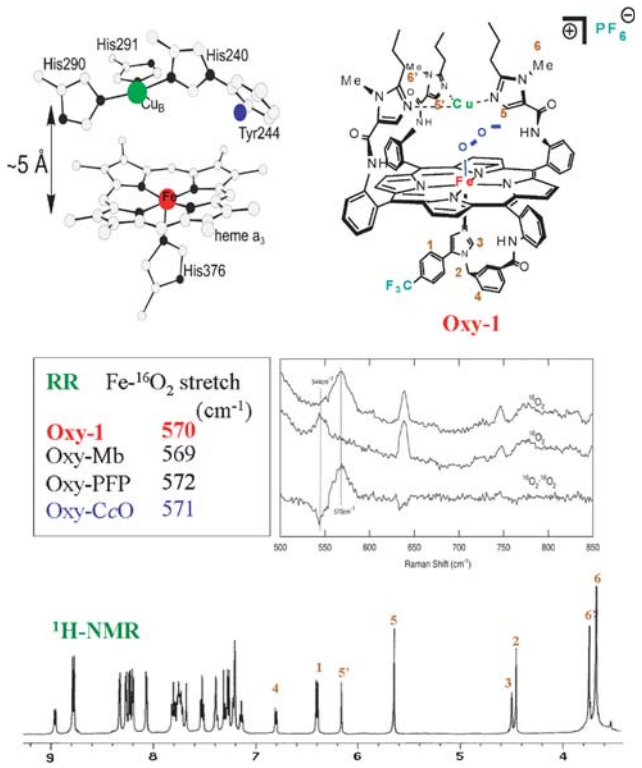

Fig. 12 Spectroscopic evidence for a heme-superoxide/Cu(I) intermediate.

oxy-myoglobin and the ''picket fence'' oxygen complex are diamagnetic because the two unpaired electrons, one on low-spin Fe(III) and the other on bound superoxide engage in a bonding interaction.[17a,b] This results in formation of a partial double bond between Fe and O, which is manifest by a higher stretching frequency. The same situation is shown by the four Resonance Raman (RR) frequencies in Fig. 12, depicted for our CcO model oxygen complex (Oxy-1),[15] oxygenated myoglobin,[17a] our ancient picket fence oxygen complex,[17b] and the oxygen complex formed by CcO itself.[16] The assignment of these frequencies were verified by substitution of ^{18}O for ^{16}O, which produced the expected isotopic shifts. Such isotopic RR shifts for our model complex are shown in the upper right-hand corner of Fig. 12.

In the presence of a neighboring redox-active phenol near the active site of CcO and our model, these oxygen complexes are unstable.[13a] We have explored this internal redox reaction, which has also been studied in CcO.[11a–g] A typical single-turnover reaction is shown in Fig. 13, where intermediate steps are proposed on the basis of resonance Raman, EPR and reactivity experiments. At −60 °C the oxygen complex is stable enough to observe its characteristic Fe–O RR frequency. Warming this complex to −40 °C results in an intramolecular redox reaction affording an Fe(IV) oxo (ferryl) group, oxidized Cu_B (which has become Cu(II)), and a phenol radical. The ferryl group was characterized by its characteristic higher-frequency RR band and oxygenation of triphenylphosphine forming the phosphine oxide. Both Cu(II) and the phenol radical were characterized by their ESR spectra.

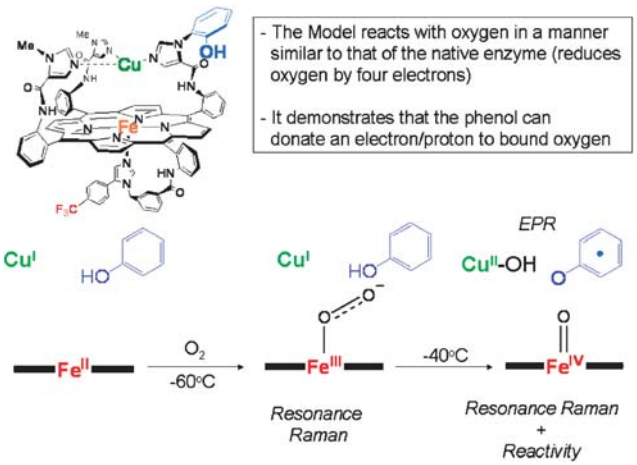

Fig. 13 Single turnover studies. Internal electron transfers minimize the lifetime of reactive intermediates.

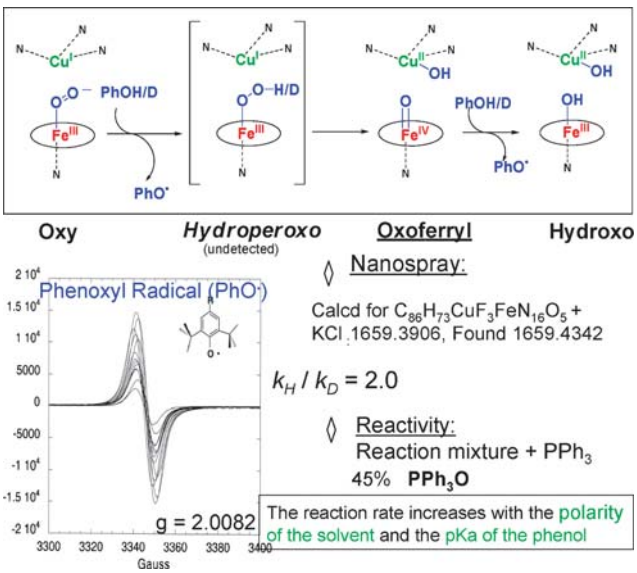

Fig. 14 Intermolecular reaction between a heme-superoxide/Cu(I) and phenols.

As shown in Fig. 14, a corresponding intermolecular redox reaction was studied by allowing an oxygen complex that lacks an internal phenol to react with a soluble hindered phenol.[13a] In this case the kinetics of the redox reaction was followed and using a deuterated phenol a small isotope effect was observed. The resulting ferryl was further characterized using high-resolution nanospray mass spectrometry. Note that excess phenol further reduces the ferryl in a subsequent step.

At this stage a putative functional model had been prepared[13b] and the internal redox reaction between the oxygen complex and Cu_B and the phenol in Tyr244 established. The next stage required developing a method to connect these functional mimics to an electron source. As shown in Fig. 15, this was accomplished using an electrode to provide the electrons. The electrochemical current can be used to follow the catalytic reduction of oxygen; moreover, the selectivity of this multi-electron reaction can be assayed by measuring any PROS that are formed during oxygen reduction. Such

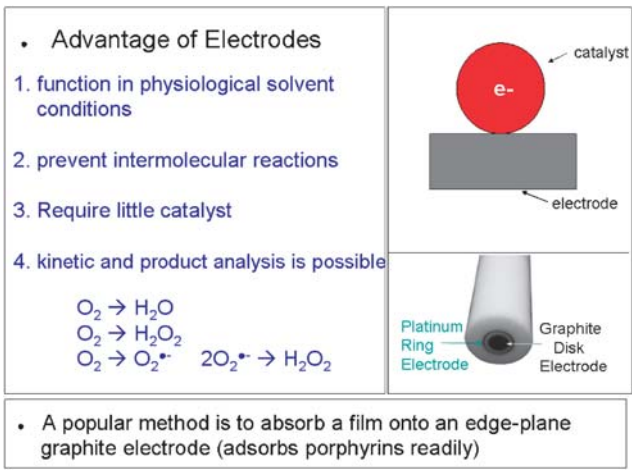

Fig. 15 Connecting structural mimics to electron sources.

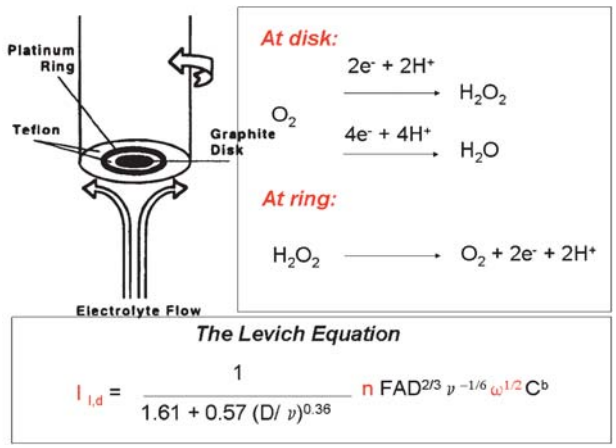

Fig. 16 Rotating ring disk electrochemistry. Parameters in the Levich equation: D, diffusion coefficient of O_2; ν, viscosity; n, number of electrons passed during O_2 reduction; F, Faraday constant; A, surface area of the electrode; ω, rotational frequency of the rotating electrode; C concentration in O_2.

electrocatalysis can be studied using a rotating ring disc electrode assembly.[18a–k] A typical porphyrin catalyst is adsorbed on a disc electrode, which is surrounded by a platinum ring electrode. As is shown in Fig. 16, oxygen is reduced at the disc and any hydrogen peroxide byproduct produced during oxygen reduction can be analyzed at the Pt ring. During the experiment the potential of the disc is swept from an initially positive potential to a more negative potential where oxygen is reduced; the Pt ring is held at a constant high positive potential, sufficient to oxidize hydrogen peroxide. The catalytic current $t > I_d$ should obey the "Levich equation",[18g,h] which can be evaluated in terms of the square root of the rotational frequency of the rotating electrode, (omega, ω), and the number of electrons (n) that are passed during the reduction of oxygen. Thus using the ring current and evaluating the data by means of the Levich equation it is possible to measure the selectivity of the catalytic reduction of oxygen. The ring currents give an independent measure of any PROS that are formed.

Attaching the catalyst to a SAM on the electrode

Previously we had published many examples of such electro-catalytic reductions of dioxygen using porphyrin catalysts adsorbed on graphite electrodes.[18a–f] However, this technique has a serious drawback for the current biomimetic study: it cannot be used under conditions where the delivery of electrons is slow and therefore rate limiting as it is in CcO. This limitation required us to develop a new electrochemical method by covalently attaching catalysts to an organic film on a gold electrode surface.[19a–d] As illustrated in Fig. 17, "SAMs", self-assembled-mono-layers are prepared by chemisorption of long chain alkyl thiols on gold disc electrodes.

The advantages of using SAM electrodes are outlined in Fig. 18. These organic films are well defined and can be easily characterized by infrared and XPS spectroscopy.[20a,b] Redox components attached to these SAM films can be diluted and therefore isolated. Most significantly, the rate of electron transfer through the SAM film to the electro-catalyst can be

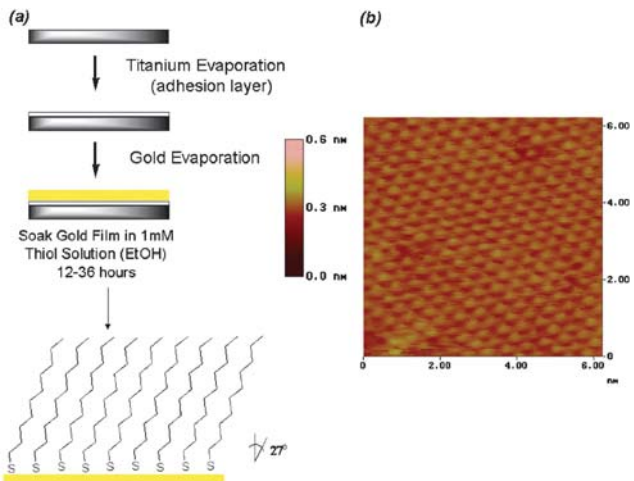

Fig. 17 "SAMs": Organic monolayers on electrodes. (a) Preparation of SAM, (b) STM image of a SAM.

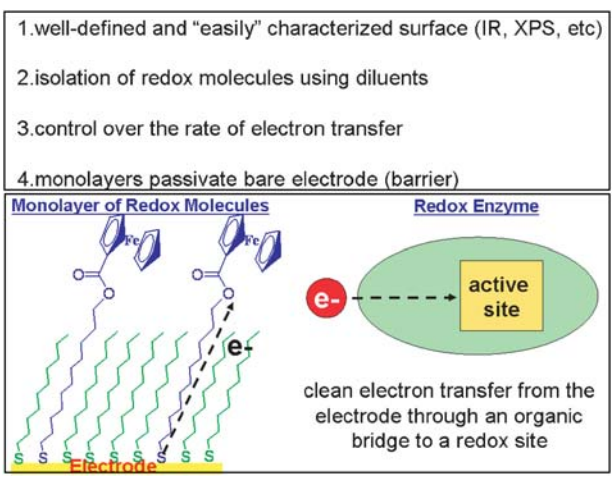

Fig. 18 Advantages of using SAM electrodes.

controlled and measured. These electron transfer rates through the hydrocarbon film depend on the lengths and chemical nature of the intervening SAM.[21] The bare electrode does not interfere because it is passivated by the SAM film. This technique was first examined by attaching ferrocenes to SAM coated gold electrodes and electrochemically measuring the rates of electron transfer through the SAM.[21]

As illustrated in Fig. 19, the next step required covalently coupling our functional CcO active site catalysts to such SAM electrode films. Coupling is superior to direct absorption. The choice of a coupling reaction is crucial. Past methods had given incomplete reaction, complex byproducts on the SAMs and involved harsh conditions.[20a,b]

A superior solution to catalyst coupling was developed by using Cu(I) catalyzed "click" chemistry pioneered by Sharpless and Meldal.[22a–c] These catalytic click reactions give nearly quantitative yields at room temperature, and work best in aqueous solution. The two "orthogonal reagents", organic azides, and terminal acetylenes do not react with themselves and show little reactivity with many reagents; but as shown in Fig. 20, under Cu(I) catalysis the organic azide and terminal acetylene groups undergo a quantitative, regio-specific 1,5-cycloaddition affording a stable triazole. We found this reaction to be an ideal method of attaching our catalyst on SAM electrodes.[19a–b,21, 23a–d] We then

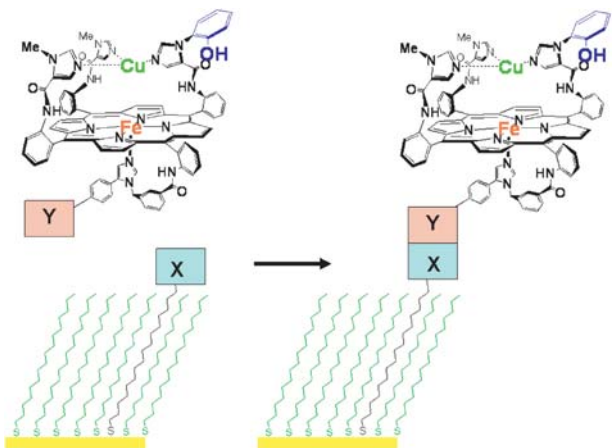

Fig. 19 Coupling of the catalyst to SAMs.

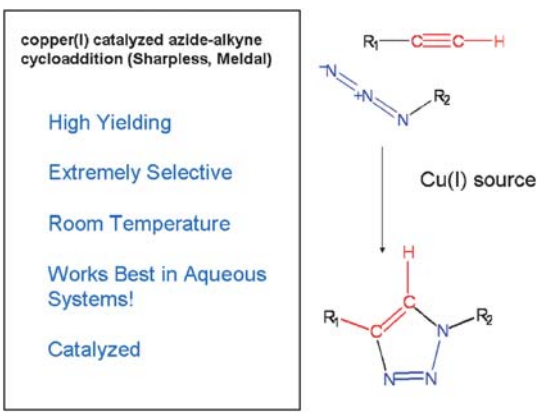

Fig. 20 "Click" chemistry.

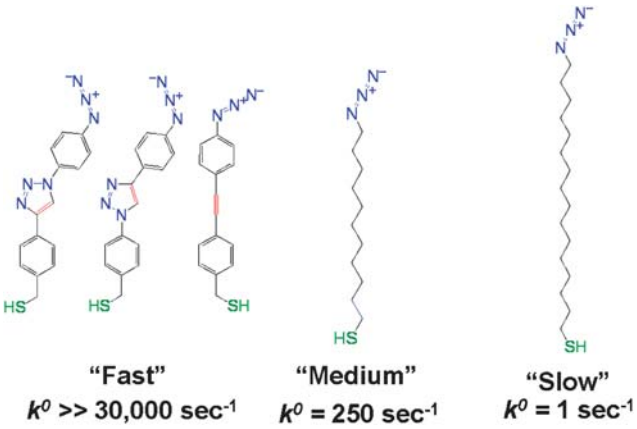

Fig. 21 Azide-terminated bridges for varying the rate of electron delivery.

developed, as shown in Fig. 21, a series of azide terminated thiols, which were used to prepare ferrocene linked SAM films and then measured the rates which electrons travel through these films to and from gold electrodes.[21] These electron transfer rates vary over an enormous range. We used the fastest and the slowest SAMs to study our functional CcO active site models during the catalytic reduction of oxygen.[19a]

As a model electro-catalytic reaction, we examined the oxidation of soluble ascorbate with SAM terminated ferrocenes. The results, shown in Fig. 22 show that with the "fast SAM" catalytic reduction of bound ferrocenium depends on the diffusion of the ascorbate to the SAM surface. In contrast, ascorbate reduces the ferrocinium linked to the "slow SAM" by a rate that is limited by the transfer of electrons from the gold electrode through the slow SAM film under steady state catalytic turnover. The latter case is analogous to the situation we wished to use with our biomimetic functional CcO catalyst, because the rate of catalytic oxygen reduction in the enzyme is limited by the arrival of electrons to CcO ;*via* diffusing Cyt c.[12a–i]

We also needed to measure the selectivity during catalytic oxygen reduction by measuring the amount of PROS that is

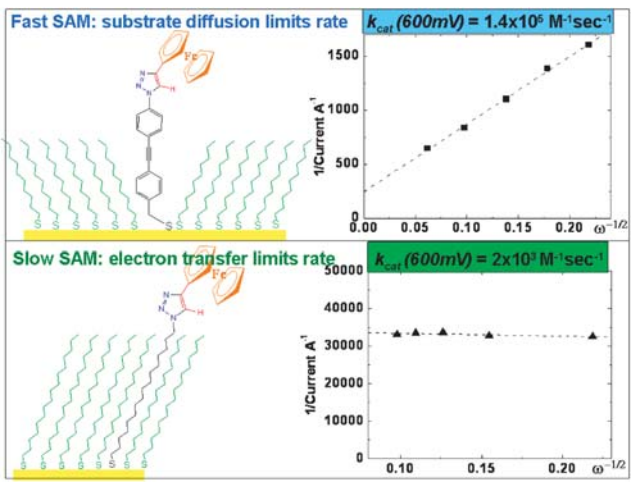

Fig. 22 The monolayer strongly influences the kinetics of the catalytic reduction of ascorbate. These results illustrate the response of a rapid electron transfer and a rate limiting electron transfer.

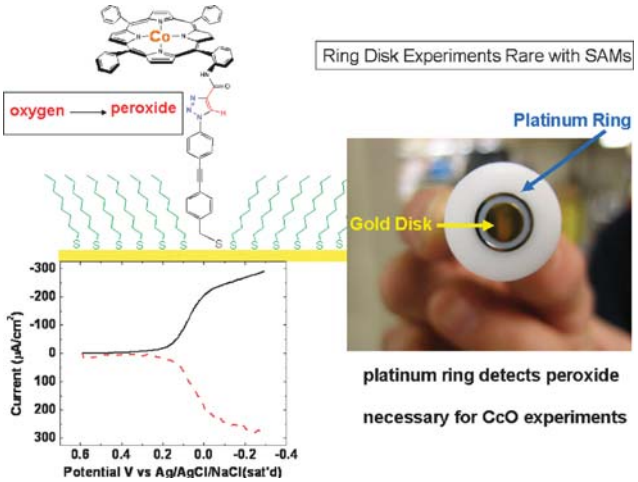

Fig. 23 Detecting peroxide from a cobalt catalyzed reduction of oxygen.

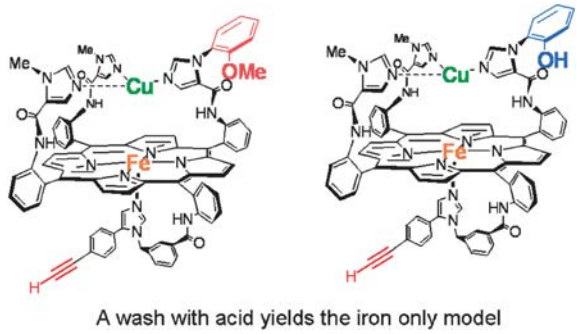

Fig. 24 Models of cytochrome c oxidase bearing a phenol (Tyr244 mimic).

produced. As shown in Fig. 23, by using the rotating ring disc technique we quantitatively measured PROS formed by using a cobalt porphyrin that had been clicked onto the fast SAM. The electrochemical results shown in the lower left hand section show that the Pt ring electrode detects the hydrogen peroxide produced by cobalt-catalyzed oxygen reduction at the disc. This was one of the first examples of an electrocatalytic reaction that has been studied on a SAM coated electrode with the rotating ring disc technique.

Now that all the techniques are in hand to study the catalytic reduction of oxygen under rate limiting electron flux, we needed to prepare catalysts that are structurally similar to the active site in CcO. As shown in Fig. 24, we required models for the active site of CcO, that have a terminal acetylene ready to be clicked onto an azide substituted SAM/gold electrode assembly.[19b] Note that the compound on the left does not have a reactive phenol because it is protected as a methyl ether. A simple acid wash of that compound removes the distal Cu forming an "Fe only" model, which we used to understand the role of Cu_B during oxygen reduction.

Synthetic strategies

This array of required functional models was challenging to prepare. The synthetic methods that we worked out over several years are outlined in Fig. 25–27 and illustrate the three phases in the synthesis of the C*c*O model. We began with a mixture of the four atropisomers of meso-tetra(*ortho*-aminophenyl)porphyrin,[24a]

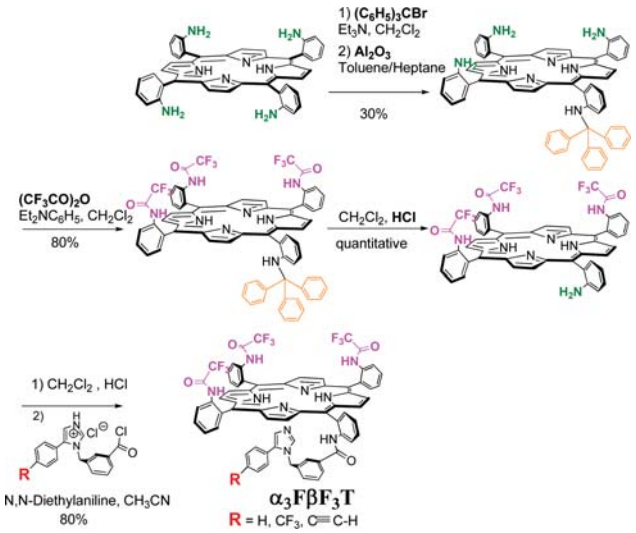

Fig. 25 Syntheses of CcO model. Face selection and insertion of the proximal imidazole.

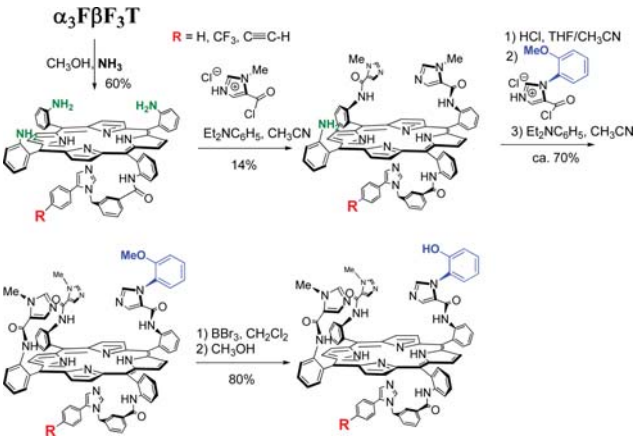

Fig. 26 Syntheses of CcO model. Appending the distal imidazoles.

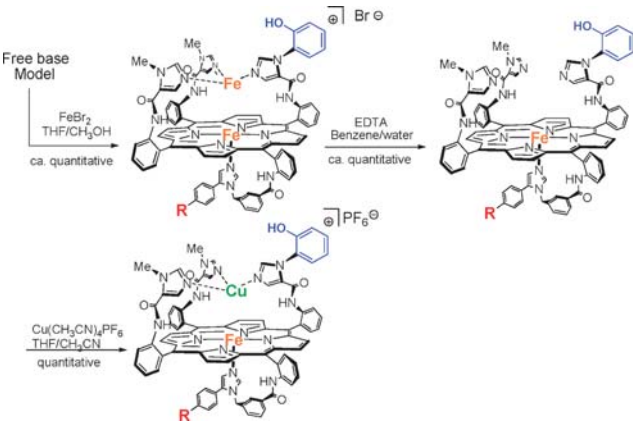

Fig. 27 Syntheses of CcO model. Metallations and demetallations.

which was then derivatized by introducing a trityl group on one of the aniline substituents.[24b] This mixture of atropisomers was heated in solution and stirred over a large plug of alumina. Slowly isomerization and adsorbtion/de-adsorbtion occurs until only one major isomer remains, adsorbed on the alumina. In this isomer three amines end up on one side of the porphyrin ring opposite to the bulky, hydrophobic trityl group, making this atropisomer adsorb most tenaciously to the alumina. During heating and stirring rotational isomerization and selective adsorption take place until only this atropisomer remains adsorbed on the alumina bed. Using this strategy, up to 5 g of this synthon can be prepared in a single batch. After washing this isomer from the alumina the three free amines were then protected with trifluoroacetyl groups. Subsequently the trityl group was removed with acid and a proximal imidazole was introduced using an imidazole-substituted acid chloride.[19a,24c,d] This synthon can possess various substituents: a CF_3 group used in ^{19}F NMR analysis (see below),[13b,24c–e] or a terminal acetylene[19a] for clicking the catalyst onto an azide-substituted SAM film.

As shown in Fig. 26, the three distal amines were subsequently deprotected with ammonia and imidazoles were attached to two of these amines, again employing imidazole acid chloride derivatives.[19b,24e] This step is delicate because one amine remains unsubstituted and *cis* and *trans* regioisomers are formed. The desired *cis*-isomer was separated using a rotating chromatotron.[19b] After reprotecting the distal imidazoles with acid, the remaining free amine was then functionalized with an imidazole acid chloride, which contains a phenol methyl or trityl ether.

The remaining steps are shown in Fig. 27. First, the trityl or methyl ether was hydrolyzed to the phenol either by acid wash for the former or using BBr_3 for the later; this step is delicate. The resulting model with a free phenol is air/light sensitive.[19b,24e] At this stage the two different metals must be introduced.[13b,19b,24d] In past work we found that all metallation steps must be carried out at the end of the synthesis, because metals interfere with organic reactions, but this restriction does not apply to click reactions. Iron was introduced using $FeBr_2$, but Fe binds to both the porphyrin and the three distal imidazole ligand set. A wash with EDTA selectively removes the unwanted distal Fe; Cu is then introduced into the distal site using a Cu(I) salt in acetonitrile. PF_6^- was used as the counter anion. This anion can be monitored using ^{19}F NMR spectroscopy and the integral of this signal can be compared with that from a CF_3 group that was previously introduced into the proximal imidazole ligand.[13b,24e] These synthetic procedures are lengthy, but convergent. It is essential that very pure catalysts be isolated; however only quite small amounts of catalysts are required for electrocatalytic experiments (micromole level).

Studies of the functional models

Two functional models of the CcO active site are shown in Fig. 28; the catalyst on the left has been clicked onto a slow SAM and the one on the right to a fast SAM. The former model is biomimetic, since electron flow from a gold electrode to the active site should be rate limiting during catalytic

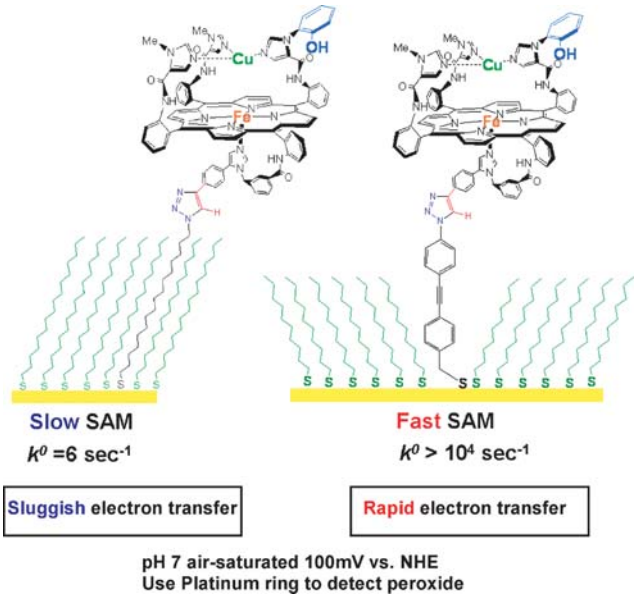

Fig. 28 CcO mimics attached to SAMs

oxygen reduction; whereas the second should exhibit a fast electron flow that is not rate limiting.

We compared the two situations under biomimetic conditions of pH 7 in an air-saturated aqueous solution using a rotating ring disc device so that PROS could be measured during catalytic reduction of oxygen.[19a]

The electrocatalytic results for these biomimetic models are summarized in Fig. 29, where the percentage of electrons lost as PROS during steady-state reduction of oxygen is compared for each of three catalysts on both the slow and fast SAM. As expected, the complete catalyst (see the blue graph on the left) attached to the biomimetic slow SAM exhibits the smallest leakage of PROS (only 4% of the electrons are lost as PROS during steady-state catalytic reduction of oxygen.[19a] But when the phenol is blocked, as shown on the green graph, 12% of the electrons are wasted forming PROS.[19a] Removal of Cu_B (the "Fe only" case) shows no catalytic activity,

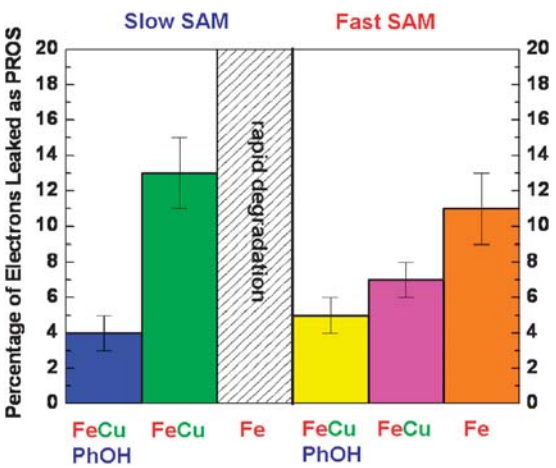

Fig. 29 The electrons that are wasted as PROS during the catalytic reduction of oxygen.

apparently because of rapid, irreversible catalyst destruction—probably by excess PROS generated during initial oxygen reduction.[19a] The data shown on the right hand side of Fig. 29 demonstrate what happens when these three catalysts are attached to a fast SAM where electrons are rapidly delivered from the electrode to the catalyst during oxygen reduction. This is an abiological situation. Under these conditions of rapid electron flux, the complete catalyst is not quite as selective (the yellow graph) as it was for the slow SAM case, but this is still a fairly selective catalyst. Masking the redox-active phenol component produces a catalyst that almost as selective (the purple graph), but this catalyst is decidedly better than the same one shown on the corresponding green graph results from the slow SAM. Even the Fe-only catalyst, which lacks both the phenol and Cu_B (the orange graph) shows moderate selectivity when electrons arrive rapidly from the electrode through the fast SAM.[19a]

The lessons gained from comparing the results shown in Fig. 29 are: under biomimetic conditions where electron flux is rate-limiting, all of the redox centers in the active site model are required for selective four-electron reduction of oxygen.[19a] However, under the abiological conditions shown for the fast SAM, where electrons are delivered rapidly from the gold electrode to the catalyst, the additional redox centers Cu_B, and the phenol are not required to affect four-electron reduction of oxygen.[19a] One can surmise that both Cu_B and the phenol are required to rapidly deliver electrons to bound oxygen when additional electrons arrive slowly at the active site, which is the situation during steady state turnover of CcO.

The complete catalyst, containing all of the redox centers present in the active site of CcO shows about 94% selectivity towards four-electron reduction of oxygen under steady state catalytic catalysis when the electron flux is rate limiting. This catalyst is still imperfect. Why? Two plausible explanations are posed in Fig. 30. Recall that in CcO both Fe*a3* and Cu_B are reduced before or near the moment that oxygen binds to heme *a3* in the active site. This apparent redox cooperativity ensures that the active site contains all of the reducing equivalents that are necessary to affect four-electron reduction, as was found in single turnover experiments.[13a,b] Our present catalyst lacks this sophisticated characteristic. Another imperfection is related to a well known side reaction: hydrolysis of the oxygen

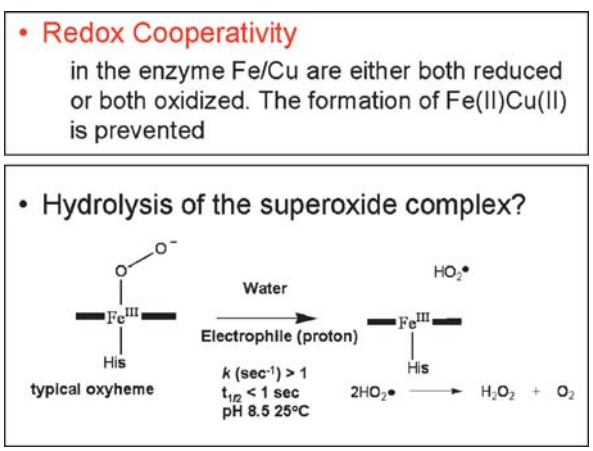

Fig. 30 The functional biomimetic model is not perfect: why?

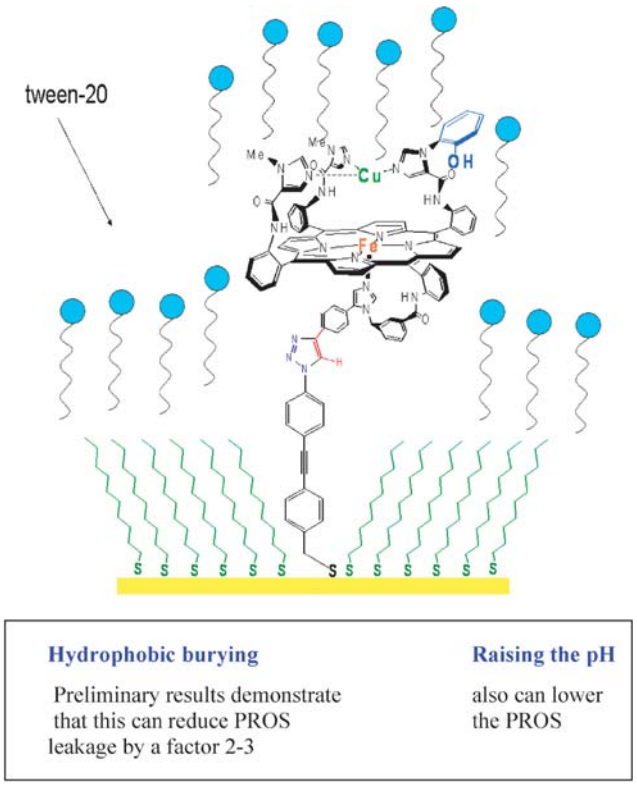

Fig. 31 Improving selectivity: toward >99%.

complex, which can be considered Fe(III)/superoxide, affords a very reactive PROS, hydroperoxyl, that decomposes into hydrogen peroxide and singlet oxygen. Typical oxygenated hemes, both natural and synthetic are known to undergo such rapid hydrolysis.[25] This reaction is promoted by electrophiles such as protons. This is undoubtedly the reason that our picket fence oxygen complex is unstable in the presence of water. As shown in Fig. 31 we have found that the PROS can be reduced by a factor of three when a hydrophobic surfactant, tween-20 is adsorbed on our catalyst, which is attached to the fast SAM. Such a surfactant layer may shield the catalyst from the aqueous environment.[18f] Raising the pH also reduces the amount of PROS, apparently by slowing down hydrolysis of the coordinated superoxide.

A delicate balance must be achieved between delivering required protons to the catalyst, slowing hydrolysis of the oxygen complex, and controlling the rate-determining electron flux to the catalyst.

Conclusions

In this research we have demonstrated that a synthetic catalyst which contains all of the essential features in CcO's active site, is able to catalytically reduce oxygen by four-electrons at physiological pH and potential, specifically under conditions of rate-limiting electron flux. This synthetic model system mimics a critical function of a essential process essential to respiration. Moreover, catalytic and single turnover experiments have provided evidence supporting a plausible mechanism for this multi-electron redox process. Further

refinement of these catalysts may yield a deeper, more precise understanding of CcO itself.

Acknowledgements

This research has been funded by NIH under grant No. 5R01 GM-17880-35 and GM-69658-R01. R. A. D. is thankful for a Lavoisier Fellowship.

Notes and references

1 (*a*) G. T. Babcock and M. Wikstrom, *Nature*, 1992, **356**, 301; (*b*) S. Ferguson-Miller and G. T. Babcock, *Chem. Rev*., 1996, **96**, 2889; (*c*) B. Ludwig, E. Bender, S. Arnold, M. Huttemann, I. Lee and B. Kadenbach, *ChemBioChem*, 2001, **2**, 392.

2 (*a*) R. E. Blankenship, *Molecular Mechanisms of Photosynthesis*, Blackwell Science, Oxford UK, 2002; (*b*) Photosystem II: The Light-DriVen Water: Plastoquinone Oxidoreductase, *Advances in Photosynthesis and Respiration 22*, ed. T.J. Wydrzynski and K. Satoh, Springer, Dordrecht, The Netherlands, 2005.

3 (*a*) I. Dance, *Chem.–Asian J*., 2007, **2**, 936; (*b*) J. B. Howard and D. C. Rees, *Chem. Rev*., 1996, **96**, 2965; (*c*) B. K. Burgess and D. J. Lowe, *Chem. Rev*., 1996, **96**, 2983; (*d*) D. C. Rees, *Biochemistry*, 1997, **36**, 1181.

4 (*a*) Other incomplete models have been reported[4*b–k*] that do not show catalytic activity; (*b*) J. A. Cappuccio, I. Ayala, G. I. Elliott, I. Szundi, J. Lewis, J. P. Konopelski, B. A. Barry and O. Einarsdottir, *J. Am. Chem. Soc*., 2002, **124**, 1750; (*c*) J.-G. Liu, Y. Naruta, F. Tani, T. Chishiro and Y. Tachi, *Chem. Commun*., 2004, 120; (*d*) E. Kim, E. E. Chufan, K. Kamaraj and K. D. Karlin, *Chem. Rev*., 2004, **104**, 1077; (*e*) J.-G. Liu, Y. Naruta and F. Tani, *Angew. Chem., Int. Ed*., 2005, **44**, 1836; (*f*) E. Kim, J. Shearer, S. Lu, P. Moënne-Loccoz, M. E. Helton, S. Kaderli, A. D. Zuberbühler and K. D. Karlin, *J. Am. Chem. Soc*., 2004, **126**, 12716; (*g*) E. Kim, K. Kamaraj, B. Galliker, N. D. Rubie, P. Moenne-Loccoz, S. Kaderli, A. D. Zuberbuhler and K. D. Karlin, *Inorg. Chem*., 2005, **44**, 1238; (*h*) E. Kim, M. E. Helton, S. Lu, P. Moenne-Loccoz, C. D. Incarvito, A. L. Rheingold, S. Kaderli, A. D. Zuberbuhler and K. D. Karlin, *Inorg. Chem*., 2005, **44**, 7014; (*i*) Y. Nagano, J. G. Liu, Y. Naruta, T. Ikoma, S. Tero-Kubota and T. Kitagawa, *J. Am. Chem. Soc*., 2006, **128**, 14560; (*j*) J. G. Liu, Y. Naruta and F. Tani, *Chem.–Eur. J*., 2007, **13**, 6365; (*k*) J. O. Baeg and R. H. Holm, *Chem. Commun*., 1998, 571.

5 (*a*) M. K. F. Wikstrom, *Nature*, 1977, **266**, 271; (*b*) K. Krab and M. Wikstrom, *Biochim. Biophys. Acta*, 1987, **895**, 25; (*c*) I. Belevich, D. A. Bloch, N. Belevich, M. Wikstrom and M. I. Verkhovsky, *Proc. Natl. Acad. Sci. USA*, 2007, **104**, 2685; (*d*) M. Wikstrom and M. I. Verkhovsky, *Biochim. Biophys. Acta*, 2007, **1767**, 1200.

6 (*a*) S. Iwata, C. Ostermeier, B. Ludwig and H. Michel, *Nature*, 1995, **376**, 660; (*b*) T. Tsukihara, H. Aoyama, E. Yamashita, T. Tomizaki, H. Yamaguchi, K. Shinzawa-Itoh, R. Nakashima, R. Yaono and S. Yoshikawa, *Science*, 1995, **269**, 1069; (*c*) T. Tsukihara, H. Aoyama, E. Yamashita, T. Tomizaki, H. Yamaguchi, K. Shinzawa-Itoh, R. Nakashima, R. Yaono and S. Yoshikawa, *Science*, 1996, **272**, 1136; (*d*) C. Ostermeier, A. Harrenga, U. Ermler and H. Michel, *Proc. Natl. Acad. Sci. USA*, 1997, **94**, 10547; (*e*) S. Yoshikawa, K. Shinzawa-Itoh, R. Nakashima, R. Yaono, E. Yamashita, N. Inoue, M. Yao, M. J. Fei, C. P. Libeu, T. Mizushima, H. Yamaguchi, T. Tomizaki and T. Tsukihara, *Science*, 1998, **280**, 1723.

7 (*a*) J. P. Abrahams, A. G. W. Leslie, R. Lutter and J. E. Walker, *Nature*, 1994, **370**, 621; (*b*) J. R. Knowles, *Annu. Rev. Biochem*., 1980, **49**, 877.

8 (*a*) T. K. Das, C. Pecoraro, F. L. Tomson, R. B. Gennis and D. L. Rousseau, *Biochemistry*, 1998, **37**, 14471; (*b*) G. Buse, T. Soulimane, M. Dewor, H. E. Meyer and M. Bluggel, *Protein Sci*., 1999, **8**, 985; (*c*) E. Pinakoulaki, U. Pfitzner, B. Ludwig and V. C. Constantinos, *J. Biol. Chem*., 2022, **277**, 13563.

9 (*a*) A. J. Moody, *Biochim. Biophys. Acta*, 1996, **1276**, 6; (*b*) J. A. Farrar, P. Lappalainen, W. G. Zumft, M. Saraste and A. J. Thomson, *Eur. J. Biochem*., 1995, **232**, 294.

10 (*a*) H. R. McLennan and M. Degli Eposi, *J. Bioenerg. Biomembr*., 2000, **32**, 153; (*b*) I. Lee, E. Bender and B. Kadenbach, *Mol. Cell. Biochem*., 2002, **234–235**, 63.

11 (*a*) G. B. Gennis, *Biochim. Biophys. Acta-Bioenerg*., 1998, **1365**, 241; (*b*) D. A. Proshlyakov, M. A. Pressler and G. T. Babcock, *Proc. Natl. Acad. Sci. USA*, 1998, **95**, 8020; (*c*) F. MacMillan, A. Kannt, J. Behr, T. Prisner and H. Michel, *Biochemistry* 1999, **38**, 9179; (*d*) A. Sucheta, I. Szundi and O. Einarsdottir, *Biochemistry*, 1998, **37**, 17905; (*e*) D. A. Proshlyakov, M. A. Pressler, C. DeMaso, J. F. Leykam, D. L. DeWitt and G. T. Babcock, *Science*, 2000, **290**, 1588; (*f*) T. Uchida, T. Mogi and T. Kitagawa, *Biochemistry*, 2000, **39**, 6669; (*g*) B. A. Barry and O. Einarsdottir, *J. Phys. Chem. B*, 2005, **109**, 6972.

12 (*a*) S. S. Gupte and C. R. Hackenbrock, *J. Biol. Chem*., 1988, **263**, 5241; (*b*) S. S. Gupte and C. R. Hackenbrock, *J. Biol. Chem*., 1988, **263**, 5248; (*c*) M. Brunori, G. Antonini, F. Malatesta, P. Sarti and M. T. Wilson, *Eur. J. Biochem*., 1987, **169**, 1; (*d*) B. Chazotte and C. R. Hackenbrock, *J. Biol. Chem*., 1989, **264**, 4978; (*e*) R. A. Capaldi, *Annu. Rev. Biochem*., 1990, **59**, 569; (*f*) B. C. Hill, *J. Biol. Chem*., 1994, **269**, 2419; (*g*) J. E. Morgan, M. I. Verkhovsky, G. Palmer and M. Wikstrom, *Biochemistry*, 2001, **40**, 6882; (*h*) R. B. Gennis, *Front. Biosci*., 2004, **9**, 581; (*i*) M. Brunori, A. Giuffre and P. Sarti, *J. Inorg. Biochem*., 2005, **99**, 324.

13 (*a*) J. P. Collman, R. A. Decreau and C. J. Sunderland, *Chem. Commun*., 2006, 3894; (*b*) J. P. Collman, R. A. Decreau, Y.-L. Yan, J. Yoon and E. I. Solomon, *J. Am. Chem. Soc*., 2007, **129**, 5794.

14 (*a*) M. Wikstrom, *Proc. Natl. Acad. Sci. USA*., 1981, **78**, 4051; (*b*) Y. Orii, *Ann. N. Y. Acad. Sci*., 1988, **550**, 105; (*c*) M. Wikstrom, *Nature (London)*, 1989, **338**, 776; (*d*) M. Wikstrom and J. Morgan, *J. Biol. Chem*., 1992, **267**, 10266; (*e*) A. A. Konstantinov, N. Capitanio, T. V. Vygodina and S. Papa, *FEBS Lett*., 1992, **312**, 71; (*f*) C. Varotsis, Y. Zhang, E. H. Appelman and G. T. Babcock, *Proc. Natl. Acad. Sci. USA*, 1993, **90**, 237; (*g*) T. Ogura, S. Takahashi, K. Shinzawa-Itoh, S. Yoshikawa and T. Kitagawa, *Bull. Chem. Soc. Jpn*., 1994, **64**, 2901; (*h*) J. E. Morgan, M. I. Verkhovsky and M. Wikström, *Biochemistry*, 1996, **35**, 12235; (*i*) M. I. Verkhovsky, J. E. Morgan and M. Wikstrom, *Proc. Natl. Acad. Sci. USA*, 1996, **93**, 12235; (*j*) A. Sucheta, K. E. Georgiadis and O. A. Einarsdottir, *Biochemistry*, 1997, **36**, 554.

15 J. P. Collman, C. J. Sunderland, K. Berg, M. A. Vance and E. I. Solomon, *J. Am. Chem. Soc*., 2003, **125**, 6648.

16 C. Varotsis, W. H Roodruff and G. T. Babcock, *J. Biol. Chem*., 1990, **265**, 11131.

17 (*a*) M. Tsubaki, K. Nagai and T. Kitagawa, *Biochemistry*, 1980, **19**, 379; (*b*) J. M. Burke, J. R. Kincaid, S. Peters, R. R. Gagne, J. P. Collman and T. G. Spiro, *J. Am. Chem. Soc*., 1978, **100**, 6083.

18 (*a*) J. P. Collman, L. Fu, P. C. Herrmann and X. M. Zhang, *Science*, 1997, **275**, 949; (*b*) J. P. Collman, M. Rapta, M. Broring, L. Raptova, R. Schwenninger, B. Boitrel, L. Fu and M. L'Her, *J. Am. Chem. Soc*., 1999, **121**, 1387; (*c*) R. Boulatov, J. P. Collman, I. M. Shiryaeva and C. J. Sunderland, *J. Am. Chem. Soc*., 2002, **124**, 11923; (*d*) J. P. Collman, R. Boulatov, C. J. Sunderland and L. Fu, *Chem. Rev*., 2004, **104**, 561; (*e*) R. Boulatov, *Pure Appl. Chem*., 2004, **76**, 303; (*f*) J. P. Collman and R. Boulatov, *Angew. Chem., Int. Ed*., 2002, **41**, 3487; (*g*) J. Koutecky and V. G. Levich, *Zh. Fiz. Khim*., 1956, **32**, 1565; (*h*) V. G. Levich, *Physiochemical Hydrodynamics*, Prentice-Hall, Englewood Cliffs, NJ, 1962.

19 (*a*) J. P. Collman, N. K. Devaraj, R. A. Decreau, Y. Yang, Y.-L. Yan, W. Ebina, T. A. Eberspacher and C. E. D. Chidsey, *Science*, 2007, **315**, 1565; (*b*) R. A. Decreau, J. P. Collman, Y. Yang, Y.-L. Yan and N. K. Devaraj, *J. Org. Chem*., 2007, **72**, 2794; (*c*) M. Broring, *Angew. Chem., Int. Ed*., 2007, **46**, 6222; (*d*) N. K. Devaraj, P. H. Dinolfo, C. E. D. Chidsey and J. P. Collman, *J. Am. Chem. Soc*., 2006, **128**, 1794.

20 (*a*) C. E. D. Chidsey and D. Loicacono, *Langmuir*, 1990, **6**, 682; (*b*) D. A. Offord, S. B. Sachs, M. S. Ennis, T. A. Eberspacher, J. H. Griffin, C. E. D. Chidsey and J. P. Collman, *J. Am. Chem. Soc*., 1998, **120**, 4478.

21 N. K. Devaraj, R. A. Decreau, W. Ebina, J. P. Collman and C. E. D. Chidsey, *J. Phys. Chem. B*, 2006, **110**, 15955.

22 (*a*) H. C. Kolb, M. G. Finn and K. B. Sharpless, *Angew. Chem., Int. Ed.*, 2001, **40**, 2004; (*b*) V. V. Rostovtsev, L. G. Green, V. V. Fokin and K. B. Sharpless, *Angew. Chem., Int. Ed.*, 2002, **41**, 2596; (*c*) C. W. Tornoe, C. Christensen and M. Meldal, *J. Org. Chem.*, 2002, **67**, 3057.

23 (*a*) J. P. Collman, N. K. Devaraj and C. E. D. Chidsey, *Langmuir*, 2004, **20**, 1051; (*b*) J. P. Collman, N. K. Devaraj, T. P. A. Eberspacher and C. E. D. Chidsey, *Langmuir*, 2006, **22**, 2457; (*c*) N. K. Devaraj, G. P. Miller, W. Ebina, B. Kakaradov, J. P. Collman, E. T. Kool and C. E. D. Chidsey, *J. Am. Chem. Soc.*, 2005, **127**, 8600; (*d*) N. K. Devaraj and J. P. Collman, *QSAR Comb. Sci.*, 2007, **26**, 1253.

24 (*a*) J. P. Collman, R. R. Gagne, C. A. Reed, T. R. Halbert, G. Lang and W. T. Robinson, *J. Am. Chem. Soc.*, 1975, **97**, 1427; (*b*) J. P. Collman, M. Broring, L. Fu, M. Rapta, R. Schwenninger and A. Straumanis, *J. Org. Chem.*, 1998, **63**, 8082; (*c*) J. P. Collman, M. Broring, L. Fu, M. Rapta and R. Schwenninger, *J. Org. Chem.*, 1998, **63**, 8084; (*d*) J. P. Collman, C. J. Sunderland and R. Boulatov, *Inorg. Chem.*, 2002, **41**, 2282; (*e*) J. P. Collman and R. A. Decreau, *C. Zhang J. Org. Chem.*, 2004, **69**, 3546.

25 (*a*) M. Momenteau and C. A. Reed, *Chem. Rev.*, 1994, **94**, 659; (*b*) K. Shikama, *Chem. Rev.*, 1998, **98**, 1357; (*c*) J. P. Collman and L. Fu, *Acc. Chem. Res.*, 1999, **32**, 455.

